ELSEVIER

Journal of Nuclear Materials 307–311 (2002) 203–211

journal of nuclear materials

www.elsevier.com/locate/jnucmat

Microstructural study of irradiated isotopically tailored F82H steel

E. Wakai [a,*], Y. Miwa [a], N. Hashimoto [b], J.P. Robertson [b], R.L. Klueh [b], K. Shiba [a], K. Abiko [c], S. Furuno [a], S. Jitsukawa [a]

[a] *Department of Effects and Analysis Material Laboratory, Japan Atomic Energy Research Institute, Tokai Research Establishment, Tokai-mura, Ibaraki-ken 319-1195, Japan*

[b] *Oak Ridge National Laboratory, P.O. Box 2008, Oak Ridge, TN 37831, USA*

[c] *Tohoku University, Sendai 980-8579, Japan*

Abstract

The synergistic effect of displacement damage and hydrogen or helium atoms on microstructures in F82H steel irradiated at 250–400 °C to 2.8–51 dpa in HFIR has been examined using isotopes of ^{54}Fe or ^{10}B. Hydrogen atoms increased slightly the formation of dislocation loops and changed the Burgers vector for some parts of dislocation loops, and they also affected on the formation of cavity at 250 °C to 2.8 dpa. Helium atoms also influenced them at around 300 °C, and the effect of helium atoms was enhanced at 400 °C. Furthermore, the relations between microstructures and radiation-hardening or ductile to brittle transition temperature (DBTT) shift in F82H steel were discussed. The cause of the shift increase of DBTT is thought to be due to the hardening of dislocation loops and the formation of α′-precipitates on dislocation loops.

1. Introduction

Ferritic/martensitic steels are candidate materials for the first wall and blanket structure of fusion reactors. In the D–T fusion reaction, the high-energy neutrons produced induce displacement damage and generate hydrogen and helium gas atoms in the materials from (n,p) and (n,α) reactions. In order to investigate the effect of hydrogen gas atoms on ferritic steels using a fission reactor, hydrogen gas atoms can be generated in F82H by doping with the ^{54}Fe isotope (F82H(^{54}Fe)). An isotopically tailored F82H(^{54}Fe) steel was fabricated [1]. Irradiation of such an alloy in a mixed-spectrum fission reactor with thermal neutrons like the high flux isotope reactor (HFIR) results in the following transmutation reactions such as reactions of ^{54}Fe(n,p)^{54}Mn and ^{54}Fe(n,α)^{52}Cr. After the HFIR irradiation, hydrogen analyses of F82H(^{54}Fe) irradiated at 250 °C to 2.8 dpa was performed by Greenwood et al. [2]. The mechanical properties in the HFIR-irradiated F82H(^{54}Fe) steel have been investigated [3–6].

The effects of neutron irradiation on tensile deformation and ductile to brittle transition temperature (DBTT) of F82H and other ferritic/martensitic steels irradiated in the target position of HFIR have been reported [7–18]. Radiation-hardening occurred mainly at irradiation temperatures lower than about 400 °C, and the shift of DBTT shift rapidly increased at irradiation temperature of 250 °C. In these results, there is a difference between the peak temperature of radiation-hardening and a maximum shift of DBTT, and the study of microstructural examination is very important. Helium and hydrogen accumulations due to transmutation and implantation in these systems of ferritic/martensitic steels have been considered as a potential cause for irradiation induced helium-embrittlement [7,10,14–16]

* Corresponding author. Tel.: +81-29 282 6563; fax: +81-29 282 5922.

E-mail address: wakai@realab01.tokai.jaeri.go.jp (E. Wakai).

0022-3115/02/$ - see front matter
PII: S0022-3115(02)01261-8

and hydrogen-embrittlement [17,18]. The swelling of F82H and the other 7–9Cr low-activation ferritic steels irradiated at 430 °C to 67 dpa in FFTF was reported in Refs. [19–21]; the smallest swelling in several ferritic/martensitic steels was F82H steel and it was 0.1%, and those of the other steels were 0.1–0.7%. Recently, the synergistic effect of displacement damage and helium production on swelling in F82H doped with an ^{10}B isotope has been examined [22,23]. The swelling of F82H steel irradiated to 51 dpa was 0.6–1.2%, depending on helium production concentration. The synergistic effect of displacement damage, helium and hydrogen production on swelling in F82H ferritic/martensitic steel under triple/dual ion beams has been reported, and the swelling increased remarkably to about 3% at 400 °C [24], but it decreases with the irradiation temperature. The study of swelling suppression has been also examined [25,26].

The purpose of the present study is to show the synergistic effect of displacement damage and hydrogen or helium atoms on microstructure in F82H steel irradiated in HFIR, using isotopes of ^{54}Fe or ^{10}B, and to examine the cause of the different temperature for the hardening and the shift of DBTT in F82H steel.

2. Experimental procedure

The chemical compositions of the F82H-std, F82H(^{54}Fe) and F82H + ^{10}B specimens used in this study are given in Table 1. The details of the preparation process for the F82H(^{54}Fe) is described in Ref. [1]. Hydrogen production in the F82H(^{54}Fe) steel irradiated to 2.8 dpa were calculated as 186 appm, by Greenwood et al. [2]. In these specimens, helium atoms about 5–10 appm will be produced by impurity boron.

Standard 3-mm-diameter TEM disks of F82H steels punched from 0.25-mm-thick sheet stock were irradiated in the HFIR target in the HFIR-MFE-JP17 capsule and the HFIR-MFE-JP12 capsule as part of the JAERI/US collaborative program. The irradiation temperatures and displacement damage were 250 °C and about 2.8 dpa for the F82H-std(1) and F82H(^{54}Fe) steels in the JP17 capsule. The irradiation temperatures were 300 and 400 °C and displacement damage was about 51 dpa for the F82H-std(2) and F82H + ^{10}B in JP12 capsule. The dpa level is based on 0.00873 dpa/MWd in the target position at 85 MW reactor power.

In order to examine the effect of helium atoms on microstructural change, He^+ irradiation was also performed at 400 °C using a model alloy of Fe–9Cr. The Fe–9Cr alloy with impurity levels less than about 0.01 wt%, which is designed as high-purity, was prepared by melting high-purity constituents in a high vacuum of 10^{-9} bar with a high frequency induction furnace. The chemical composition of high-purity Fe–9Cr alloys was 9.1Cr–3ppmC–3ppmN–51ppm–2ppmS. The specimen was normalized at 1050 °C for 1.8×10^3 s in vacuum followed by an oil-quench and then tempered at 850 °C for 3.6×10^3 s in vacuum. The TEM specimen was polished using a Tenupol twin-jet system in a solution of 95 ml acetic acid and 5 ml perchlolic acid at 15 °C. He^+ ion irradiation was performed at 400 °C to a dose of 3.5×10^{19} He^+/m^2 at 15 kV.

After irradiation, microstructures of these specimens were examined using JEM-2000FX or HF-2000 transmission electron microscope operated at 200 kV.

3. Results and discussion

3.1. Pre-irradiation microstructures of the F82H-std, F82H(^{54}Fe) and F82H + ^{10}B

The microstructure after normalizing and tempering was a lath martensitic structure in both the F82H-std, F82H(^{54}Fe) and F82H + ^{10}B steel, and the microstrucutres are very similar. Large precipitates of $M_{23}C_6$ carbides with number density about 3×10^{20} m^{-3} and the mean size of about 70 nm was observed in the matrix and on grain boundaries in these steels. The number density and mean size of MC carbide in F82H(^{54}Fe) were 2×10^{20} m^{-3} respectively, and those in F82H-std and F82H + ^{10}B were 12 nm, and $<1 \times 10^{20}$ m^{-3} and 14 nm, respectively. The dislocation densities in the

Table 1
Chemical compositions of the specimens used in this study (wt%), and F82H-std(1) and F82H-std(2) was prepared for JP17 and JP12 capsules, respectively

Alloys	Cr	B	C	N	P	S	Al	Si	V	Mn	Ta	W
F82H-std(1)	7.46	0.0004	0.094	0.002	0.003	0.003	0.019	0.09	0.18	0.07	0.03	2.1
F82H-std(2)	7.44	0.0008	0.1	–	–	–	–	0.14	0.20	0.49	0.04	2.0
F82H(^{54}Fe)	7.1	–	0.097	0.007	<0.002	0.0015	0.03	0.55	0.15	0.40	0.04	1.8
F82H + ^{10}B	7.23	0.0058	0.098	–	–	–	–	0.17	0.22	0.50	0.04	2.1

F82H-std: normalizing/1040 °C, 0.67 h, tempering/740 °C, 2 h, F82H(^{54}Fe): normalizing/1040 °C, 0.33 h, tempering/745 °C, 0.67 h, F82H + ^{10}B: normalizing/1040 °C, 0.67 h, tempering/740 °C, 1.5 h.

steels were nearly equal and were about 9×10^{13} m^{-2}. The mean widths of the lath boundaries in the steels were about 450 nm.

3.2. Standard F82H and F82H(^{54}Fe) steels irradiated at 250 °C to 2.8 dpa

Fig. 1(a)–(c) show microstructures of the F82H-std steel irradiated at 250 °C to 2.8 dpa; these micrographs were taken in the [0 0 1] direction using $\mathbf{g} = 110$ at a low- and high-magnification of bright-field (BF) image condition, and a high-magnification of weak beam dark-field (WBDF) image condition, respectively. Dislocation loops were observed on {1 1 1} planes with $(\mathbf{a}/2)\langle 1\,1\,1\rangle$ Burgers vectors. Some loops were arranged along dislocation lines. The number density and mean size of the loops were 1.4×10^{22} m^{-3} and 7.9 nm, respectively. Precipitates with contrast like α′-phase were observed on many dislocation loops as indicated by arrows in Fig. 1(c). A few MC carbides were observed in the matrix. No cavities were observed in F82H-std.

In high Cr ferritic/martenstic steels containing >12% chromium, it is well known that α′-precipitates were formed in the matrix by irradiation [27]. However, in low Cr ferritic alloys with about 9% chromium, α′-precipitates were not formed in the matrix and they were formed on dislocation loops in Fe–9Cr irradiated by 1 MeV electron irradiation [28,29]. The α′-precipitates formed on dislocation loops were identified by the measurement of the distance between Moire fringe on loops. The contrast of α′-precipitates on dislocation loops were also formed in the Fe–9Cr irradiated by neutron irradiation [8,9], and the contrast of α′-precipitates on dislocation loops was very similar to that in F82H steel in this study. Therefore, it is considered that the formation of α′-precipitates on dislocation loops in low Cr ferritic steels containing about 9%Cr is a general phenomenon occurred in irradiated ferritc alloys at low temperature region.

Fig. 2(a) and (b) show microstructures of the F82H(^{54}Fe) steel irradiated at 250 °C to 2.8 dpa, and the micrographs were also taken from the [0 0 1] direction using $\mathbf{g} = 110$ at a high-magnification of BF image and WBDF image condition, respectively. Two types of dislocation loops were observed: those on {1 1 1} planes with $(\mathbf{a}/2)\langle 1\,1\,1\rangle$ Burgers vectors and those on {1 0 0} planes with $\mathbf{a}\langle 1\,0\,0\rangle$ ones. The concentration of $\langle 1\,1\,1\rangle$ type to all loops was about 73%. The total number densities and mean size of dislocation loops were 2.1×10^{22} m^{-3} and 6.6 nm, respectively. Precipitates by contrast like α′-phase were also observed on many dislocation loops and not in the matrix. A few MC carbides were observed in the matrix. In Fig. 3, small cavities were observed in F82H(^{54}Fe), and the number density, root mean cube of radius, and swelling of cavities were 5×10^{19} m^{-3}, 1.9 nm and 0.0001%, respectively.

The produced hydrogen atoms with high concentration in F82H steel irradiated in an isotopically tailored experiment affected on Burgers vector types of dislocation loops and somewhat the nucleation and growth of dislocation loops, and also the formation of the cavities. Recently, the effect of hydrogen atoms on microstructures in F82H under triple/dual ion irradiation has been examined, and it is also found that hydrogen atoms affect strongly on microstructural evolutions in F82H below 400 °C.

3.3. Microstructures of F82H-std and F82H + ^{10}B steels irradiated at 300 °C to 51 dpa

Fig. 4(a)–(c) give microstructures of the F82H-std steel irradiated at 300 °C to 51 dpa. Many dislocation loops and $M_{23}C_6$ and MC carbides were also observed. The small black contrast seen inside the $M_{23}C_6$ carbides

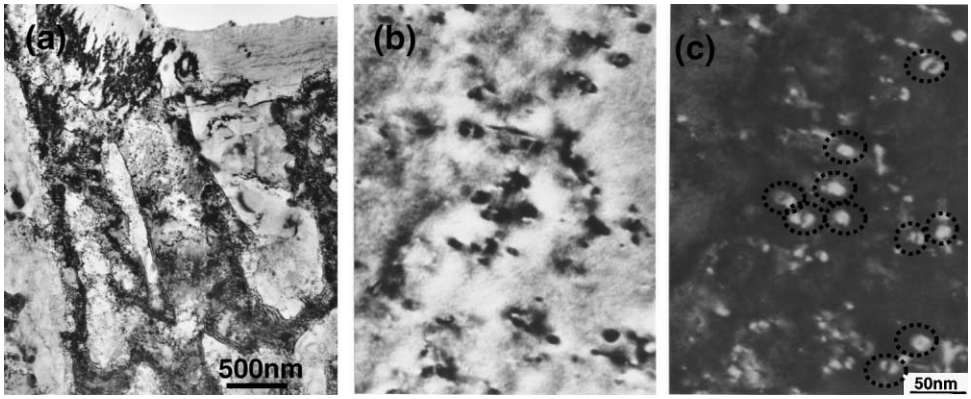

Fig. 1. Microstructures of (a) a BF image in low-magnification, (b) a BF image in high-magnification, and (c) a WBDF image in high-magnification in the F82H-std steel irradiated at 250 °C to 2.8 dpa. Precipitates with contrast like α′-phase are seen on many dislocation loops.

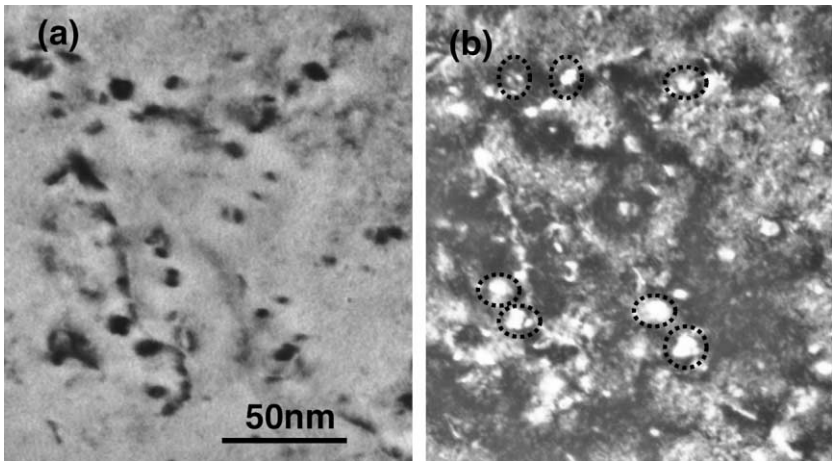

Fig. 2. Microstructures of (a) a BF image in high-magnification and (b) a WBDF image in high-magnification in the F82H(^{54}Fe) steel irradiated at 250 °C to 2.8 dpa. Precipitates with contrast like α′-phase are also seen on many dislocation loops.

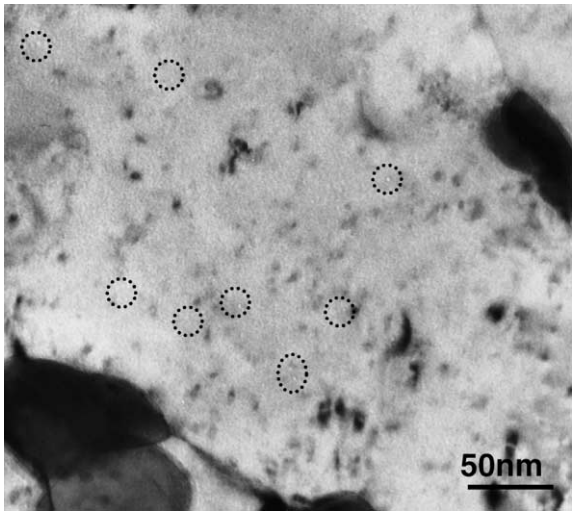

Fig. 3. Cavities formed in F82H(^{54}Fe) irradiated at 250 °C to 2.8 dpa. (Cavities indicated by dotted circles.)

is identified as M_6C precipitates, which are formed by the irradiation, and an example of a dark-field image of the M_6C precipitates is shown in Fig. 4(c). The size of the M_6C particles was 3–9 nm. The size of $M_{23}C_6$ carbide in F82H-std was nearly equal to that before irradiation. Fig. 5 shows the microstructure of F82H + ^{10}B steel irradiated at 300 °C to 51 dpa. The mean size and number density of dislocation loops in F82H-std and F82H + ^{10}B steels were about 11 nm and 4×10^{22} m^{-3} and about 11 nm and 6×10^{22} m^{-3}, respectively. The number density of loops formed in F82H + ^{10}B steel was slightly increased than that in F82H-std. These were larger and higher number density than those irradiated at 250 °C to 3 dpa. The mean size and number density of MC carbides in both alloys were about 10 nm and 1×10^{21} m^{-3}, respectively. Small cavities with mean diameter of 2.6 nm and number density of 2.4×10^{21} m^{-3} were formed in the F82H + ^{10}B steel as shown in Fig. 5(b), but not formed in F82H-std.

The produced helium atoms in F82H irradiated in an isotopically tailored experiment affected somewhat on the formation of dislocation loops and cavities. The influence of helium atoms would be small, because the mobility of helium and vacancy atoms was relatively low at 300 °C.

The formation of M_6C in the matrix during irradiation was reported in studies of F82H and the other ferritc/martensitic steels irradiated at 420 and 490 °C in FFTF [30]. M_6C consisted mainly of Ta, W and a small amount of V and Ti, and the size was smaller than $M_{23}C_6$ carbide. In the thermal aging experiments for the F82H steel, no formation of M_6C and MC precipitates was observed below 400 °C. The formation of M_6C precipitates in the matrix was also observed in 9Cr–1MoVNb and 9Cr–1MoVNb–2Ni steels irradiated at 400 °C to 37 dpa in the HFIR, but no formation of M_6C precipitates were observed in the alloys irradiated at 300 °C [31,32]. It was mentioned that the M_6C phase was Cr-rich and that Cr supersaturation or segregation during irradiation might play a role for the phase transformation. In another report, M_6C carbides in several ferritic–martensitic alloys, HT9, FV448, and 1.4914 formed along dislocation lines during irradiation at 460 °C to 50 dpa [33]. In the present experiments, M_6C precipitates formed even at 300 °C, and the precipitates were not in the matrix but instead, formed on the $M_{23}C_6$ carbides. Judging from these results, M_6C precipitates are likely to form at elevated irradiation temperatures, and the M_6C may be somewhat easier to form in the F82H than in the 9Cr–1MoVNb and the

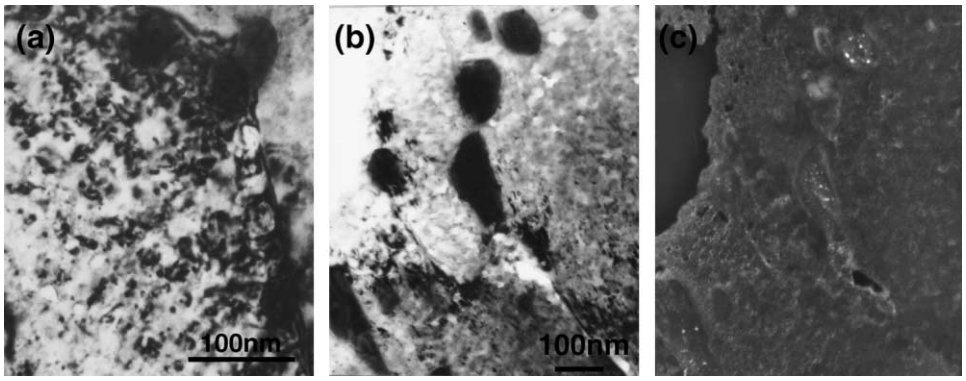

Fig. 4. Microstructures of F82H-std irradiated at 300 °C to 51 dpa: (a) dislocation loops; (b) BF image of $M_{23}C_6$, (c) DF image of M_6C.

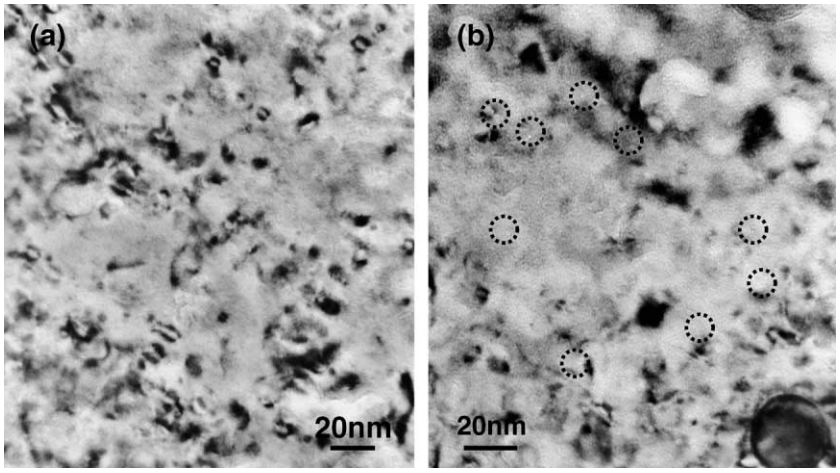

Fig. 5. Microstructures of F82H + ^{10}B irradiated at 300 °C to 51 dpa: (a) dislocation loops; (b) cavities.

9Cr–1MoVNb–2Ni steels. The formation mechanism of M_6C precipitates on the $M_{23}C_6$ carbides is not clear now, and it may be related to radiation-induced segregation of solute atoms at the surface of $M_{23}C_6$ carbides. Further detailed examination will be necessary to understand it.

3.4. Microstructures of F82H-std and F82H + ^{10}B steels irradiated at 400 °C to 7.4 and 51 dpa

Many dislocation loops and cavities were observed in F82H-std steel irradiated at 400 °C to 8 dpa as given in Fig. 6(a). No contrast of precipitates on dislocation loops was observed in F82H-std. The number density and mean size of dislocation loops in F82H-std steel irradiated to 7.4 dpa were 6×10^{21} m^{-3} and 33 nm, respectively. In 51 dpa, many dislocation loops disappeared as seen in Fig. 6(b). The number density and mean size of dislocation loops formed in F82H-std to 51 dpa were 6.5×10^{20} m^{-3} and 27 nm, respectively. The number density and the volume-averaged diameter of cavities and swelling in F82H-std steel irradiated to 7.4 dpa were 15.2 nm, 9.0×10^{20} m^{-3} and 0.17%, respectively, and these values at 51 dpa were 25.4 nm, 6.1×10^{20} m^{-3} and 0.52%, respectively.

As proceeded the irradiation, the number density of dislocation loops in the F82H-std remarkably decreased, and dislocations increased slightly before irradiation. Many dislocation loops were grown up during the irradiation between 7.4 and 51 dpa, and they could be tangled, and some parts of tangled dislocations might have disappeared at lath boundaries.

Many $M_{23}C_6$ carbides elongated along lath boundaries at 51 dpa. In Fig. 7, the elongated $M_{23}C_6$ carbides are shown, and black dotted contrast of M_6C carbides can be seen in them. M_6C carbides were mainly formed on $M_{23}C_6$ carbides and a few part of M_6C was formed in the matrix.

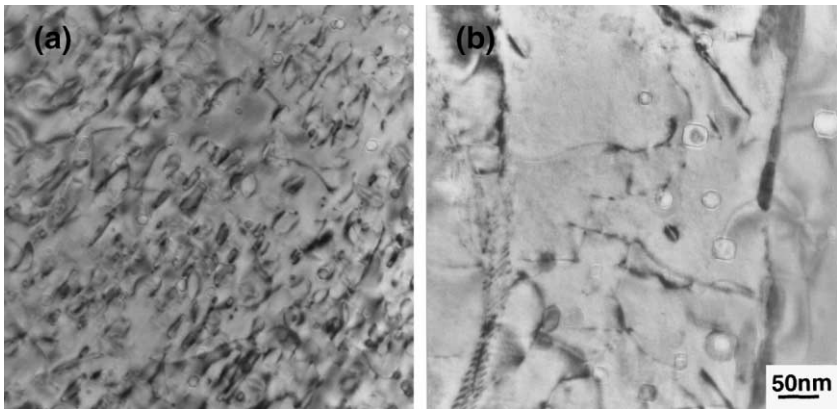

Fig. 6. Dislocation loops and cavities formed in F82H-std irradiated at 400 °C to (a) 8 dpa and (b) 51 dpa.

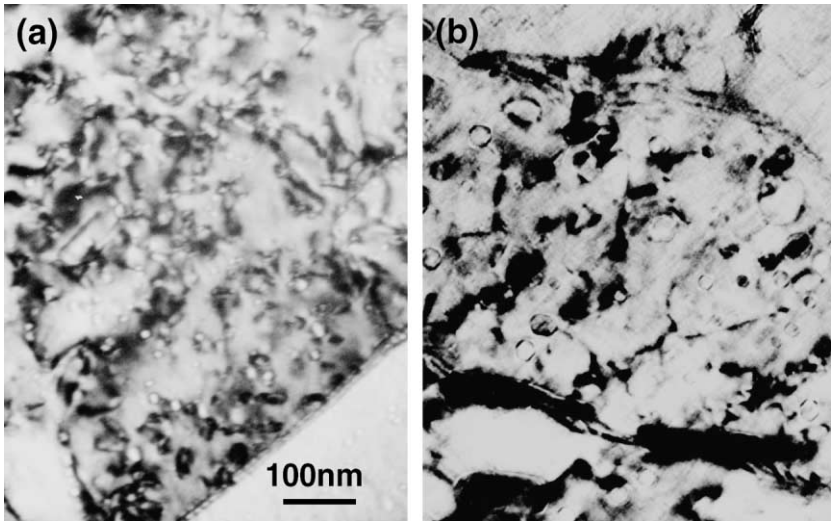

Fig. 7. Dislocation loops and cavities formed in F82H + ^{10}B irradiated at 400 °C to (a) 8 dpa and (b) 51 dpa.

Fig. 8 shows microstructures F82H + ^{10}B steel irradiation to 7.4 and 51 dpa at 400 °C. The number density of dislocation loops in F82H + ^{10}B irradiated to 7.4 dpa were about 1×10^{21} m^{-3} and about 20 nm, respectively. At 51 dpa, the number density of dislocation loops decreased and they grew. The number density and mean size of dislocation loops were about 2×10^{20} m^{-3} and about 70 nm, respectively. The dislocation density was slightly higher than that before irradiation. The number density and the volume-averaged diameter of cavities in F82H + ^{10}B irradiated to 7.4 dpa were 1.1×10^{20} m^{-3} and 6.3 nm, respectively. At 51 dpa, the number density, volume-averaged diameter of cavities and swelling were 6×10^{20} m^{-3}, 25.4 nm and 1.1%, respectively.

The produced helium atoms in F82H irradiated in an isotopically tailored experiment at 400 °C enhanced remarkably on the growth of cavity and swelling and also slightly the formation of dislocation loops, but the growth of dislocation loops was suppressed.

At 400 °C, α′-precipitates on dislocation loops could not be formed in the F82H-std and F82H + ^{10}B steels. The cause of no formation of α′-precipitates may be related with the temperature below the phase boundary between α′-phase and α-phase in F82H during irradiation.

In Fig. 9, the effect of helium atoms on the formation of α′-precipitates on dislocation is shown using an Fe–9Cr alloy irradiated at 400 °C by He^+ ions. In the previous study, α′-precipitates were formed on dislocation loops in Fe–9Cr irradiated at 400 °C by 1 MeV electron irradiation. However, no formation of α′-precipitates on dislocation loops was observed, and helium atoms suppressed the formation of α′-precipitates. The reason can

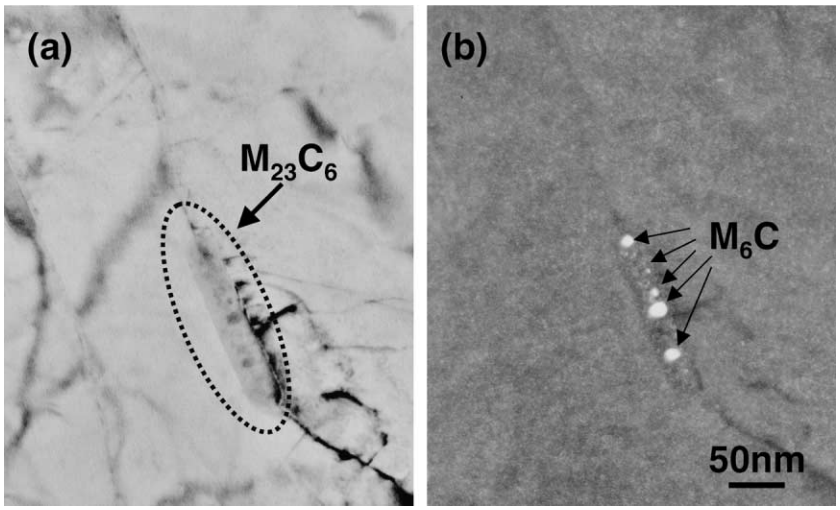

Fig. 8. (a) BF image of M_6C and $M_{23}C_6$. (b) DF image of M_6C in F82H-std irradiated at 400 °C to 51 dpa.

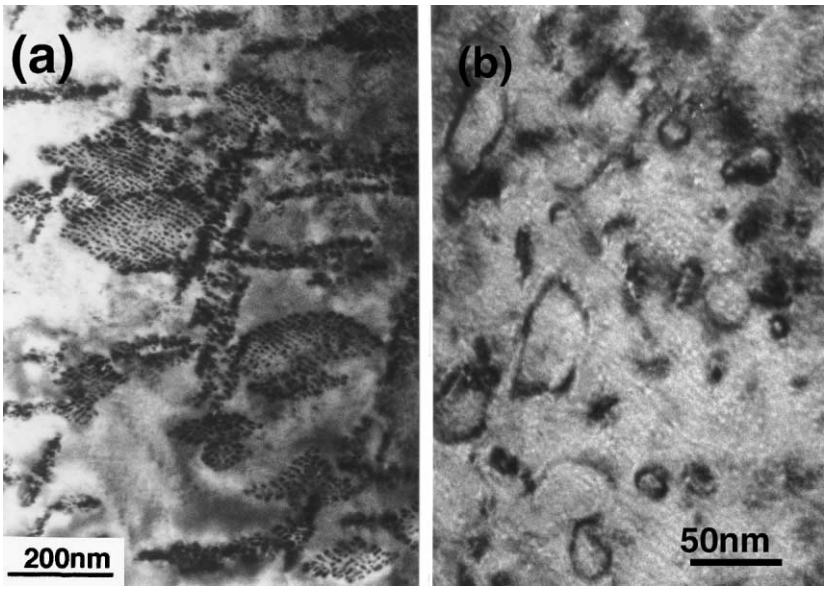

Fig. 9. Dislocation loops formed in Fe–9Cr alloy: (a) 1 MeV electron irradiation; (b) 15 keV He^+ irradiation. α′-precipitates were formed on dislocation loops by the electron irradiation.

be explained by the idea that the strong binding between helium and vacancy atoms degrades chromium segregation to dislocation loops. Therefore, helium atoms would have an effect of suppression of α′-precipitate formation.

3.5. Radiation-hardening and embrittlement

Many data of tensile properties of yield strength in F82H and the other ferritic/martensitic steels showed that radiation-hardening rapidly decreased at 400 °C, and the hardening was nearly equal at temperatures between 200 and 350 °C. However, the shift of DBTT decreased rapidly at 350 °C, and it increasing with decreasing irradiation temperature below 350 °C. There was incompatibility for correlation between the temperature of increase of radiation-hardening and the maximum shift of DBTT. Below 350 °C, many dislocation loops were formed, but the number density and mean size of dislocation loops were very similar. At 250 °C, many α′-precipitates were formed on dislocation loops. Considering this results, the hardening can be

similar below about 300 °C form the model of estimation for the increase of yield strength caused by microclusters, based on the Orowon's theory for athermal bowing of dislocations around obstacles on a slip plane, and this is summarized by Bement [34] as described below: The contributions from each short range obstacles are described as follows:

$$\Delta\sigma_i = M\alpha\mu b(N_i d_i)^{1/2},$$

where M, α, μ, b, N_i, and d_i are Tayor factor, barrier strength of i-kind of obstacles, the shear modulus of matrix, the Burger's vector of moving dislocation, the number density of the obstacles, and the mean diameter of the obstacle, respectively. Microstructural study of defect clusters formed by the irradiation at 250–400 °C showed that the cause of increase of the shift of DBTT is thought to be due to not only the hardening of dislocation loops but also the formation of α'-precipitates on dislocation loops.

4. Summary

To examine the relation between radiation-hardening or embrittlement and microstructures in ferritic/martensitic steels, the microstructures of reduced-activation F82H steel irradiated in HFIR at 250–400 °C to 2.8–51 dpa were examined by TEM. The microstructures of Fe–9Cr alloy irradiated by neutrons, electrons and He^+ ions. respectively, were also examined. The obtained results are described as below;

(1) A few small cavities were formed in F82H doped with ^{54}Fe(F82H(^{54}Fe)) steel irradiated at 250 °C to 2.8 dpa, but the swelling is insignificant, while in the F82H-std steel no cavities were observed. In this irradiation temperature, precipitates with contrast similar to the α'-phase were observed on many dislocation loops. The number density and mean size for dislocation loops in the F82H-std and F82H(^{54}Fe) steels are 1.4×10^{22} m^{-3} and 7.9 nm, and 2.1×10^{22} m^{-3} and 6.6 nm, respectively. The types of loops are $\mathbf{b} = (\mathbf{a}/2)\langle 1\,1\,1\rangle$ for the F82H-std and $\mathbf{b} = (\mathbf{a}/2)\langle 1\,1\,1\rangle$ and $\mathbf{a}\langle 100\rangle$ for the F82H(^{54}Fe) steel. The concentration of $\mathbf{a}\langle 1\,1\,1\rangle$ type to all loops in the F82H(^{54}Fe) steel is about 73%.

(2) In F82H steel irradiated at 300 °C to 51 dpa, many dislocation loops with $\mathbf{b} = (\mathbf{a}/2)\langle 1\,1\,1\rangle$ were formed and the number density and mean size of them were 4×10^{22} m^{-3} and 11 nm, respectively. The precipitates contrast similar to α'-phase was somewhat observed on dislocation loops.

(3) In F82H irradiated at 400 °C to 8 dpa, dislocation loops and cavities were formed. No precipitate contrast was observed on dislocation loops. The number density and mean size of dislocation loops were 6×10^{21} m^{-3} and 33 nm, respectively. The number density and the volume-averaged diameter of cavities were 1×10^{21} m^{-3} and 15 nm, respectively. As proceeded the irradiation to 51 dpa at 400 °C, the number density of dislocation loops decreased to 6.5×10^{20} m^{-3} and the dislocation density was slightly increased. The number density and the volume-averaged diameter of cavities were 6×10^{20} m^{-3} and 25.4 nm, respectively.

(4) Furthermore, the relations between microstructures and radiation-hardening or DBTT shift in F82H steel were discussed. The cause of increase of the DBTT shift is thought to be due to not only the hardening of dislocation loops but also the formation of α'-precipitates on dislocation loops.

Acknowledgements

The authors would like to thank Drs A.F. Rowcliffe and S.J. Zinkle in Oak Ridge National Laboratory and members of Radiation Effect Analyses Laboratory in Japan Atomic Energy Research Institute for fruitful discussions. We are also grateful to Messrs L.T. Gibson, A.T. Fisher, and J.J. Duff, and the members of the Irradiated Materials Examination and Testing Laboratory of ORNL for technical supports.

References

[1] M. Suzuki, A. Hishinuma, N. Yamonouchi, M. Tamura, A.F. Rowcliffe, J. Nucl. Mater. 191–194 (1992) 1056.
[2] L.R. Greenwood, B.M. Oliver, S. Ohnuki, K. Shiba, Y. Kohno, A. Koyama, J.P. Robertson, J.W. Meadows, D.S. Gelles, J. Nucl. Mater 283–287 (2000) 1438.
[3] M.L. Hamilton, D.S. Gelles, S. Ohuki, K. Shiba, Y. Kohno, A. Koyama, Fusion Reactor Materials, DOE/ER-0313/25, p. 136.
[4] D.S. Gelles, M.L. Hamilton, B.M. Oliver, L.R. Greenwood, Fusion Reactor Materials, DOE/ER-0313/25, p. 143.
[5] E. Wakai, N. Hashimoto, J.P. Robertson, L.R. Kleuh, K. Shiba, S. Jitsukawa, Fusion Reactor Materials, DOE/ER-0313/25.
[6] D.S. Gelles, M.L. Hamilton, B.M. Oliver, L.R. Greenwood, Fusion Reactor Materials, DOE/ER-0313/27, p. 149.
[7] R.L. Klueh, M.A. Sokolov, K. Shiba, Y. Miwa, J.P. Robertson, J. Nucl. Mater. 283–287 (2000) 478.
[8] E. Wakai, A. Hishinuma, K. Usami, Y. Kato, S. Takaki, K. Abiko, Mater. Trans., JIM 41 (9) (2000) 1180.
[9] E. Wakai, A. Hishinuma, T. Sawai, Y. Kato, S. Isozaki, S. Takaki, K. Abiko, Phys. Stat. Sol. (a) 160 (1997) 441.
[10] K. Shiba, A. Hishinuma, J. Nucl. Mater. 283–287 (2000) 474.
[11] K. Shiba, I. Ioka, J.P. Robertson, M. Suzuki, A. Hishinuma, Euromat 96 (1996) 265.
[12] A.F. Rowcliffe, J.P. Robertson, R.L. Klueh, K. Shiba, D.J. Alexander, M.L. Grossbeck, S. Jitsukawa, J. Nucl. Mater. 258–263 (1998) 1275.

[13] S.J. Zinkle, J.P. Robertson, R.L. Klueh, Fusion Reactor Materials Semiannual Progress Report for Period Ending 30 June 1988, Office of Fusion Energy, DOE/ER-0313/24, p. 135.
[14] E.I. Materna-Morris, M. Rieth, K. Ehrlich, Effects of radiation on materials, STP 1366, 2000, p. 597.
[15] M. Rieth, B. Dafferner, H.-D. Röhrig, J. Nucl. Mater. 258 (1998) 1147.
[16] N. Yamamoto, J. Nagakawa, K. Shiba, J. Nucl. Mater. 283–287 (2000) 400.
[17] Y. Dai, S.A. Maloy, G.S. Bauer, W.F. Sommer, J. Nucl. Mater. 283–287 (2000) 513.
[18] N. Baluc, R. Schäublin, C. Bailat, F. Paschoud, M. Victoria, J. Nucl. Mater. 283–287 (2000) 731.
[19] A. Kimura, M. Narui, H. Kayano, J. Nucl. Mater. 191–194 (1992) 879.
[20] T. Morimura, A. Kimura, H. Matsui, J. Nucl. Mater. 239 (1996) 118.
[21] A. Kimura, H. Matsui, J. Nucl. Mater. 212–215 (1994) 701.
[22] E. Wakai, N. Hashimoto, Y. Miwa, J.P. Robertson, L.R. Klueh, K. Shiba, S. Jitsukawa, J. Nucl. Mater. 283–287 (2000) 799.
[23] Y. Miwa, E. Wakai, K. Shiba, N. Hashimoto, J.P. Robertson, A.F. Rowcliffe, A. Hishinuma, J. Nucl. Mater. 283–287 (2000) 334.
[24] E. Wakai, T. Sawai, K. Furuya, A. Naito, T. Aruga, K. Kikuchi, S. Yamashita, S. Ohnuki, S. Yamamoto, H. Naramoto, S. Jistukawa, these Proceedings.
[25] T. Sawai, E. Wakai, K. Tomita, A. Naito, S. Jistukawa, in: Proceedings of the 10th International Conference on Fusion Reactor Materials, Germany, 2001.
[26] E. Wakai, T. Sawai, A. Naito, S. Yamashita, S. Ohnuki, S. Jistukawa, J. Nucl. Mater., in press.
[27] A. Kimura, H. Matsui, J. Nucl. Mater. 212–215 (1994) 701.
[28] E. Wakai, A. Hishinuma, K. Yano, S. Takaki, K. Abiko, J. Physique (IV) 5 (C7) (1995) 277.
[29] E. Wakai, A. Hishinuma, Y. Kato, S. Takaki, K. Abiko, in: K. Abiko, K. Hirokawa, S. Takaki (Eds.), Proceedings of the Ultra High Purity Base Metals, The Japan Institute of Metals Sendai, Japan, 1994, p. 522.
[30] T. Shibayama, A. Kimura, H. Kayano, Euromat 96 (1996) 533.
[31] P.J. Maziasz, J. Nucl. Mater. 169 (1989) 95.
[32] P.J. Maziasz, R.L. Klueh, J.M. Vitek, J. Nucl. Mater. 141–143 (1986) 927.
[33] P. Dubuisson, D. Gilbon, J.L. Seran, J. Nucl. Mater. 205 (1993) 178.
[34] A.L. Bement Jr., in: Proceedings of the Second International Conference on Strength of Metals and Alloys, ASM Metals Park, OH, 1970, p. 693.